



An Effective Osteogenesis Cryogel γ -PGA/HEMA/PEG Served as Rabbit Orbital Bone Defects Scaffolds*

XIONG Ke^{1,2)}, LIU Chun-Tao¹⁾, WU Zhao-Ying¹⁾, ZHANG Wei^{3)**}, ZHANG Chao^{1)**}

¹⁾School of Biomedical Engineering, Sun Yat-sen University, Shenzhen 518107, China;

²⁾Department of Ophthalmology, Nanfang Hospital, Southern Medical University, Guangzhou 510515, China;

³⁾Department of Outpatient, The First Affiliated Hospital, Sun Yat-sen University, Guangzhou 510080, China)

Abstract Objective Orbital bone fracture has become very common in recent years, and its related treatments and therapies aim at repairing the defects. Mineralized poly (γ -glutamic acid)/2-hydroxyethyl methacrylate/poly(ethylene glycol) (γ -PGA/HEMA/PEG) polymeric cryogel is a new type of scaffolding material with an interconnective porous structure. The study aimed to examine its efficacy in the repair of orbital bone defects. **Methods** The γ -PGA/HEMA/PEG polymeric cryogel was prepared by the cryogelation technique. Orbital bone defects were prepared on twenty-four New Zealand white rabbit. Three groups were made depending on the implanted materials: (1) blank control group; (2) polymeric cryogel group (Gel group); (3) mineralized polymeric cryogel group (M-gel group). Specimens were taken 8 weeks and 16 weeks after implantation for gross observation, micro-computed tomography (μ -CT) and hard tissue grinding slices and tissue sections were used to observe the osteogenesis outcome. **Results** Radiographic results showed that the mineralized cryogel could effectively facilitate the repair of the orbital bone defect completely, with the defective area completely replaced by bone tissue. Histological results proved that the mineralized polymeric cryogel scaffolds could increase the expression of runt-related transcription factor 2 (Runx-2), alkaline phosphatase (ALP), osteopontin (OPN), and platelet endothelial cell adhesion molecule-1 (CD31), which indicated the strengthened angiogenesis and osteogenic capability after the mineralized cryogel transplantation. **Conclusion** The mineralized polymeric cryogel served as a potential engineering scaffold in the repair of orbital bone defects *via* angiogenesis and osteogenesis.

Key words repair, orbital bone fracture, polymeric cryogel scaffolds, mineralization, osteogenesis

DOI: 10.16476/j.pibb.2022.0309

The orbit is a vital structure that not only could protect the eyeball but also help maintain normal eye function. It is composed of seven non-weight-bearing bones: the frontal, lacrimal, ethmoid, sphenoid, zygomatic, maxillary, and palatine. The edge of the orbital bone is irregular in shape, and it participates in shaping the lineament. The application of external stress on the cancellous orbital bone could easily create fracture at the weakest position, leading to the orbital defect. The purpose of the treatment of the orbital fracture is to repair the orbital bone defect^[1-2].

At present, the most common method in clinical treatment is to implant the repair materials, such as natural materials or artificial materials^[3-4]. Cancellous

bone is a commonly used form of autogenous bone grafting and it has outstanding performance in terms of osteoconduction, osteoinduction, and osteogenesis. But the autogenous bone also has boundedness, for example, the resources of the autogenous bone are limited, and may have the risk of bleeding, infection,

* This work was supported by grants from the Key-Area Research and Development Program of Guangdong Province (2020B090924004) and The National Natural Science Foundation of China (81971760).

** Corresponding author.

ZHANG Wei. Tel: 86-13556159255, E-mail: zhang8@mail.sysu.edu.cn

ZHANG Chao. Tel: 86-13751865819,

E-mail: zhchao9@mail.sysu.edu.cn

Received: July 1, 2022 Accepted: July 28, 2022

and chronic pain. Allogeneic bone has a wider source and provides good osteoconduction, but bad osteoinduction and osteogenesis. In addition, the allogeneic bone also has the risk of HIV or hepatitis B and the potential of immunological rejection^[5-8]. The limited availability of autogenous bone and allogeneic bone has become one of the major obstructions in clinical practice. So there is an urgent need to find a new graft that features well in histocompatibility and biomechanics and has the characteristics of osteoconduction, osteoinduction, and osteogenesis. Synthetic materials are employed as alternative bone substitutes to repair a large-scale range of orbital bone defects, such as hydroxyapatite (HA), high-density polyethylene (HDPE), calcium phosphate cement, *etc*^[9-12].

Synthetic hydrogels have been extensively utilized as scaffolding materials in bone repair/regeneration^[13]; however, the widely studied inert hydrogels are not able to induce appreciable mineralization that is essentially important for osteoinduction and osteogenesis. To this end, studies have been performed to improve the binding affinity between hydrogels and minerals^[14]. For example, it was reported that the modification of poly(2-hydroxyethyl methacrylate) (pHEMA) with carboxyl groups could effectively increase the deposition of calcium^[15]. Substrates containing biomimetic mineral-nucleating amino acid ligands could also effectively control the morphology of the mineral, some studies have indicated that crosslinked poly(γ -glutamic acid) (γ -PGA) was shown to induce the heterogeneous nucleation of hydroxyapatite *in vitro*^[16-17]. In addition, insufficient mass transportation condition of hydrogel, which is characterized by a closed porous structure, may hinder the three-dimensional homogenous mineralization inside the hydrogel scaffold; scaffolds with interconnective open-pores may better satiate the need for mineralization as well as cell migration/proliferation.

Polymeric cryogel is fabricated through the cryogelation technique, and is marked by excellent permeability due to its unique inter-connective porous structure; in addition, polymeric cryogel could be easily functionalized to offer appreciable protein adsorption and cell adhesion, and has demonstrated to be prominent scaffolding materials in the regeneration of bone, cartilage, neuron, and liver, *etc*^[18]. The

inter-connective porous structure of polymeric cryogel enables fast transportation of nutrients, oxygen, and metabolite. In terms of bone tissue engineering, physical mixing of the cryogel with bioactive minerals or mineralization of the cryogel may endow polymeric cryogel with osteoinductivity and/or osteoconductivity. In recent years, polymeric cryogel has shown great potential in the repair of defects of limb bone with good osteoinductivity and osteogenic capability^[19]. Our previous report has polymeric cryogel can induce osteogenic differentiation of rMSC by activating the BMP/Smad and the FAK-ERK1/2 signaling pathways^[20-22].

In this work, we introduced γ -PGA into the hydroxyethyl methacrylate/ethylene glycol(HEMA/PEG) backbone to prepare a co-polymer cryogel, namely, methacrylate poly(γ -glutamic acid)/hydroxyethyl methacrylate/poly(ethylene glycol) diacrylate (γ -PGA/HEMA/PEG) cryogel. Then, the γ -PGA/HEMA/PEG cryogel was mineralized *in vitro* to form a mineralized cryogel. To assess the therapeutic potential of mineralized polymeric cryogel scaffolds for orbital bone defect repair, we analyzed its angiogenic and osteogenesis ability *in vitro*. In addition, the three dimensional-computed tomography (3D-CT) reconstruction and micro-CT (μ CT) analysis were applied to analyze the defect repair efficiency *in vivo*. These mineralized polymeric cryogel scaffolds would effectively facilitate the regeneration of critical-sized orbital defects in a rabbit orbital defect model. We hypothesized that the mineralized polymeric cryogel scaffolds could boost the orbital defect repair through the angiogenic and osteogenesis dual-lineage effect (Figure 1).

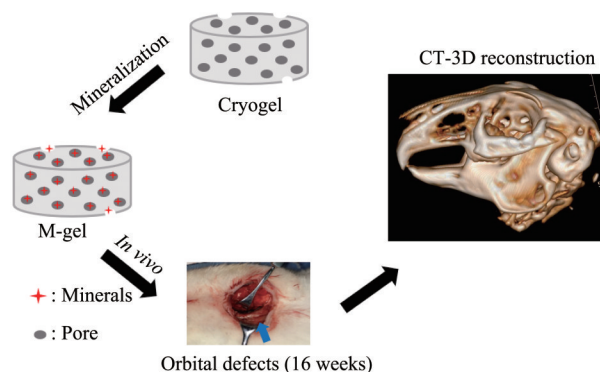


Fig. 1 Schematic illustration of the mineralized polymeric cryogel scaffolds repairs rabbits orbital bone defects

1 Materials and methods

1.1 Materials

Methacrylate poly (γ -glutamic acid) (mPGA, molar mass 1.0×10^6 g/mol, 10.0% of degrees of substitution of methacryloyl groups), and poly (ethylene glycol) diacrylate (PEGDA, molar mass 3 400 g/mol, degrees of substitution of acryloyl groups of 97.5%) were synthesized following previous reports^[23-24]. Phosphate-buffered saline (PBS), simulated body fluid (SBF), and 40 mmol/L Ca^{2+} /24 mmol/L HPO_4^{2-} immersion solution were prepared according to the established protocols^[17, 25]. Tetramethylethylenediamine (TEMED, Aladdin Industrial Co.), 2-hydroxyethyl methacrylate (HEMA, 98%, Aladdin Industrial Co.), and ammonium persulphate (APS, Guangzhou Chemical Reagent Factory, China) were used as received. Other chemicals in this study were of analytical grade and were applied without further purification.

1.2 Fabrication of polymeric cryogel scaffolds

γ -PGA/HEMA/PEG cryogel was fabricated according to previously reported methods^[21], using phosphate-buffered saline containing 1.0 mol/L of sodium chloride as the reaction media. Briefly, a

solution of 0.1% (w/v) of mPGA, 5% (w/v) of PEGDA_{3.4k}, and 10% (w/v) of HEMA in the reaction media were chilled to 4°C. To this solution, 0.1% (v/v) of TEMED and 0.5% (w/v) of APS were orderly added and vortexed. A certain amount of the mixture solution was quickly transferred to a plastic straw as the mold and polymerized at -20°C for 8 h, and then at -16°C for 72 h. After the cryogelation, the product was thawed in deionized water and placed in the shaker (100 r/min) at 25°C for 24 h, the deionized water was for three times to remove the residual monomer, precursor, and initiator. For *in vitro* mineralization, the cryogel was autoclaved and equilibrated in sterile phosphate-buffered saline for 24 h; then the materials were immersed in 40 mmol/L Ca^{2+} /24 mmol/L HPO_4^{2-} solution for 3 h, followed by incubation in simulated body fluid for 16 h, and then in fresh simulated body fluid for another 16 h. The mineralized cryogel in this study were the products after two immersion processes. The mineralized polymeric cryogel scaffolds were presented as M-gel, and the non-mineralized polymeric cryogel scaffolds were termed Gel in the following context. The final products were storage at normal temperature (Figure 2).

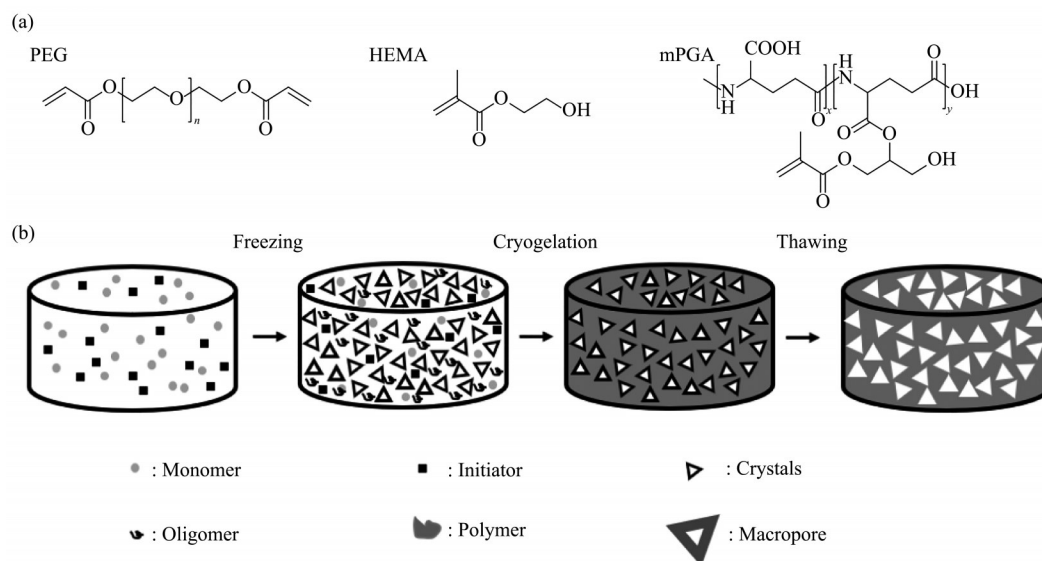


Fig. 2 The structures of PEGDA, HEMA & mPGA (a) and the process of cryogel preparation (b)

1.3 Characterization of polymeric cryogel scaffolds

The chemical structures of the cryogels or

mineralized cryogels were confirmed by Fourier transform infrared (FT-IR) spectroscopy. The materials were homogenized and lyophilized. The

spectra were recorded over a range of 4 000–400 cm^{-1} with the Bruker Vertex 70 spectrometer (Bruker, Germany). The acquired dry powder was compressed into a thin film and analyzed with the Rigaku X-ray diffractometer (Cu $\text{K}\alpha 1$) (energy: 36 kV, current: 30 mA, rotating rate: $4^\circ/\text{min}$, and angular range (2θ): 5° – 80°).

Equilibrium water content (EWC) of the polymeric cryogel scaffolds was measured gravimetrically using the following equation^[22]:

$$\text{EWC}/\% = [(M_s - M_d) / M_d] \times 100 \quad (1)$$

Where M_s and M_d are the weight of the swollen cryogel and the dry cryogel respectively.

The porosity of the cryogel was calculated according to Archimedes' principle using a gravity bottle. Briefly, first, the dry weight of cryogel sample was recorded, followed by soaking the cryogel sample in cyclohexane filled in a specific gravity glass bottle and recording the submerged weight of the cryogel sample. The cryogel was then taken out and the weight of the cryogel (containing cyclohexane in the void volume) was recorded. The values taken at each step were substituted in the given equation to calculate the porosity of the cryogel.

$$\text{Porosity}/\% = (M_w - M_d) / (M_w - M_{\text{sub}}) \times 100 \quad (2)$$

Where M_w is cyclohexane saturated cryogel. M_d is the dry mass of the cryogel and M_{sub} is the submerged mass of the cryogel.

Freeze-dried cryogels ($n=4$) with known mass (M_d) were immersed in PBS in a water bath at 37°C under mild shaking, and the solution was changed every 48 h. Samples were taken out at a predetermined time points (0, 2, 4, 6, 8, 12, and 16 weeks), washed with ultra-pure water 10 times to remove the residual enzymes and degradation products, air-dried, and weighed (M_{dt}). The mass loss rate was calculated according to the following equation:

$$\text{Mass loss rate}/\% = (1 - W_{dt}/W_d) \times 100 \quad (3)$$

The cross-sections of the cryogel were observed, briefly, and the paraffin sections of cryogel (thickness: 10 μm) were prepared using a microtome, stained with Alizarin red, and photographed digitally under a light microscope ($\times 7$; Olympus, Tokyo, Japan). The pore size of the cryogel was measured manually using image analyzing software (Image-Pro plus 6.0, Media Cybernetic, Silver Springs, MD, USA).

On account of the dimensions of these cryogel

reductions after drying, lyophilization was performed for purpose of obtaining the correct morphological information. The cryogel samples were prepared from the monoliths, which were vacuum-dried at -50°C using a lyophilizer (Martin Christ GmbH, Germany). The gold coating of the cryogel was performed by mounting them on the base plate of a sputter coater (Vacuum Tech, Bangalore, India). The topographical structure of the cryogel was examined by scanning electron microscope (SEM, Thermal field emission environmental SEM-EDS-EBSD, Quanta 400 FEG, FEI/OXFORD/HKL, France) at a high vacuum (20 kV) with a spot size of 3.5–4.5 mm varied from sample to sample.

Minerals in the mineralized cryogel were measured by Scanning electron microscopy-energy dispersive spectroscopy (SEM-EDS). Calcium deposition in cryogel was also stained with Alizarin Red S and analyzed under the optical microscope. The swollen cryogels ($n=6$) were trimmed into a disc shape with diameter of 6 mm and height of 4 mm for uniaxial static compression test at a strain rate of 0.1 mm/min on an LR10KPlus mechanical analyzer (LLOYD, UK)^[22].

1.4 Rabbit model establishment of repair of orbital bone defects

In the present study, a total of 24 five-month-old New Zealand white rabbits (bodyweight 2.0–3.0 kg, Center of Experimental Animals, Southern Medical University, Guangzhou, China) were randomized into three groups ($n=8$ in each group)^[26]. To build the orbital bone defect, the rabbits were anesthetized with intramuscular droperidol (0.25 mg/kg), intravenous pentobarbital (20 mg/kg), and general 2% isoflurane (v/v), in a lateral decubitus position. When skin preparation and draping were completed, muscle along the inferior margin eyelid was cut horizontally. The operation region was marked with the methylene blue pen, then the bone tissue (12 mm) along the inferior margin of the orbit was cut off with an electro-saw. Because the inferior margin of the orbit is mainly composed of the zygomatic bone, the bone defect model of zygomatic bone (length: 12 mm, width: 6 mm, and thickness: 2 mm) was built on all of the 24 rabbits and then randomized into three groups: Group A, self-control group without any treatment (Control group); Group B, which was the treatment group with non-mineralized polymeric cryogel scaffolds (Gel

group); Group C, which was the treatment group with mineralized polymeric cryogel scaffolds (M-gel group). After bleeding was stopped with a gelatin sponge, corresponding prepared implants were implanted into the orbital defect sites to fill the whole area. Subsequently, a 5/0 suture was employed to suture the incision on the skin. The three groups of rabbits were kept in different cages in the SPF laboratory. There is no material pull-out, migration, or incision infection during the period of feeding. The protocols of animal study were authorized by the Committee on Ethics of Animal Experiments of Southern Medical University and carried out according to the institutional guidelines (No. NFYY-2019-73).

1.5 Micro-CT analysis

Experimental rabbits were sacrificed at 8 and 16 weeks postoperatively. The separated cranium was scanned with μ CT. The specimens were harvested and fixed in 4% of paraformaldehyde for 48 h. The bone microstructure of orbital bone was analyzed using μ CT (SkyScan 1176 μ -CT system, Bruker, USA) (resolution: 18 μ m, tube voltage: 80 kV, and a tube current: 313 μ A). Bone morphometric parameters, including the bone volume to sample volume (BV/TV), the number of bone trabeculae per mm of tissue (Tb. N), the trabecular thickness (Tb. Th), and the bone mineral density (BMD) were analyzed and calculated based on the region of interest (ROI) of the orbital bone defect. The technician conducting the scan analysis was unaware of the treatments associated with the specimens^[27-28].

1.6 CT 3D reconstruction

To investigate the gross morphologies, the samples were scanned using CT and reconstructed into 3D images. Orbital CT scan was performed under anesthesia before sacrifice at 16 weeks with Philips Brilliance scanners (Philips, Netherlands). CT images were reconstructed with a slice thickness of 1 mm and a 512 \times 512 matrix. CT images were preprocessed via the bone window setting (W : 1 500 HU, L : 450 HU) and resampling resample to isotropic 1 mm voxels. The 3D reconstruction technique was used to visualize the degree of orbital defect repair.

1.7 Histological analysis

The isolated orbital bone of each group was processed for histology and immunohistochemistry. Hematoxylin and eosin (H&E) staining of histological

slices was carried out at room temperature to observe the new bone regeneration conditions. Tissue samples were fixed in 4% paraformaldehyde and stored for 24 h, then decalcified with 10% EDTA solution for 3 weeks at room temperature and embedded in paraffin before being sectioned, and sliced into 5- μ m-thick transverse sections following the standard method using a rotary microtome (RM2255, Leica, Hamburg, Germany). ALP is a marker for early osteocytic differentiation, in addition, Runx-2 and OPN are important expressions of osteogenesis-related proteins. Then the slices were incubated with primary antibodies against Runx-2, ALP, and OPN at 4°C overnight according to established protocol. After staining, the histological sections were viewed on the optical microscope (DM5000B, Leica, Germany) under a bright field.

1.8 Immunofluorescence double staining

The sections assessed by immunofluorescence were blocked by incubation with 5% (w/v) BSA, incubated with primary antibodies for Anti-CD31 antibody (Abcom, ab7388), SMA skeletal muscle actin monoclonal antibody (Thermo Fisher, AB_10984949), incubated with corresponding secondary antibodies conjugated to Alexa Fluor[®] 647 and Alexa Fluor 488 fluorescent dye (Abcom, ab150167, and Thermo Fisher, AB_2534069). Immunofluorescence staining of CD31 and α -SMA was used to assess the angiogenesis of tissue. Sections were visualized with the fluorescent microscope (IX71 Olympus, Tokyo, Japan).

For the analysis of CD31 expression in the orbital bone defect area, defect area tissues were collected from sacrificed experimental rabbits by removing the tissue around the bone. To obtain a single-cell suspension, the whole samples were digested for 30 min with collagenase at 37°C. The cells were counted and incubated at 4°C for 45 min after filtration and washing. And then, cells were washed and further incubated with APC-conjugated CD31 (R&D Systems, FAB3628A) antibodies for 45 min at 4°C. The acquisition was performed on a FACScan cytometer (BD Immunocytometry Systems, USA) for demarcating and analyzing of CD31 positive cells.

1.9 Statistical analysis

One-way ANOVA tests were used to detect distinctions between groups. A P -value of less than

0.05 ($P < 0.05$) was considered statistically significant. Data were analyzed using SPSS 22.0 statistical software (IBM, USA) and presented as mean \pm SD. Significance level was presented as either * $P < 0.05$ or ** $P < 0.01$.

2 Results

2.1 Characterization of polymeric cryogel scaffolds

The fabrication and physicochemical characterization of the polymeric cryogel scaffolds has been reported in terms of EWC, porosity, pore diameter, and compressive modulus (Table 1). After mineralization, the EWC of mineralized polymeric cryogel scaffolds reduced to (87.3 \pm 0.5)% compared with that of the non-mineralized group (89.0 \pm 0.9)%; and the porosity of mineralized polymeric cryogel scaffolds (66.2 \pm 1.7)% was slightly lower than the non-mineralized group (68.6 \pm 0.3)%; no obvious changes in the pore diameter between mineralized (53.0 \pm 35.6) μ m and non-mineralized (62.6 \pm 45.6) μ m polymeric cryogel scaffolds was observed. Moreover, due to the minerals deposition, the compressive modulus of mineralized polymeric cryogel scaffolds largely increased to (42.4 \pm 1.6) kPa, which was almost twice as much as that of the non-mineralized group (21.1 \pm 0.1) kPa.

Table 1 Physical properties of cryogels

Samples	EWC/%	Pore diameter / μ m	Porosity/%	Compressive modulus/kPa
Gel	89.0 \pm 0.9	62.6 \pm 45.6	68.6 \pm 0.3	21.1 \pm 0.1
M-Gel	87.3 \pm 0.5	53.0 \pm 35.6	67.7 \pm 0.8	42.4 \pm 1.6

SEM scanning displayed the pore structure of the polymeric cryogel scaffolds. Compared with non-mineralized polymeric cryogel scaffolds, the interconnectivity of mineralized polymeric cryogel scaffolds was maintained with a small variation in the structure of the pores. The highly inter-connective structure was retained after the mineralization of cryogel under SEM. Abundant cells were observed adhered to the surface of the mineralized polymeric cryogel scaffolds, compared with the non-mineralized group (Figure 3a).

In the mineralized polymeric cryogel scaffold group, the whole section was stained red. It indicated

the minerals were deposited homogeneously in the polymeric cryogel scaffolds. Alizarin red S staining confirmed the deposition of minerals inside the pores of the scaffolds after the mineralization process (Figure 3b).

In the Fourier transform infrared spectroscopy (FTIR) spectra image, we can find the disappearance of the peak for the C=C bond (\sim 1 600 cm^{-1}) and the appearance of the amide peaks (\sim 1 650 cm^{-1} and \sim 1 550 cm^{-1}). It indicated that γ -PGA was successfully incorporated into the matrix of cryogel *via* a covalent bond. After mineralization, the intensity of peaks (\sim 963 cm^{-1} and \sim 1 036 cm^{-1}) from the backbone of the polymeric matrix scaffolds diminished greatly, while the bands of PO_4^{3-} groups appeared. Moreover, CO_3^{2-} groups had been also successfully incorporated into the minerals (\sim 870 cm^{-1}) (Figure 3c).

In the X-ray diffraction (XRD) patterns, the prominent intensity of three peaks (22 $^\circ$, 26 $^\circ$, and 33 $^\circ$) in the mineralized polymeric cryogel scaffolds has similar to hydroxyapatite (Figure 3d). The presence of Ca and P in the minerals was identified by SEM-EDS, the Ca/P ratios on the surface of the mineralized polymeric cryogel scaffolds were 1.57, which was close to that of hydroxyapatite (1.67) (Figure 3e).

The mass changes of the cryogel scaffolds during degradation are shown in Figure 4, where the non-mineralized polymeric cryogel scaffolds and the mineralized scaffolds were slowly degraded with immersion time. At 16 weeks, the mass loss rate of the non-mineralized cryogel scaffolds was (5.7 \pm 1.6)%; and that of the mineralized cryogel scaffold was (20.8 \pm 2.6)%, which is much higher than the non-mineralized ones.

2.2 Microstructure analysis of the new bone tissue

The microstructure analysis was carried out on the newly formed bones in the orbital defect sites using the CTAn software (V1.14.4) (Figure 5). The BV/TV, Tb. N, Tb. Th, and BMD of newly formed bones in the polymeric cryogel scaffold groups (Group B & C) was significantly increased, compared with the control blank group ($P < 0.05$). It indicated that polymeric cryogel scaffolds promoted bone regeneration in bone defect repair. Additionally, compared with the non-mineralized cryogel group, the bone volume of newly formed bones in the

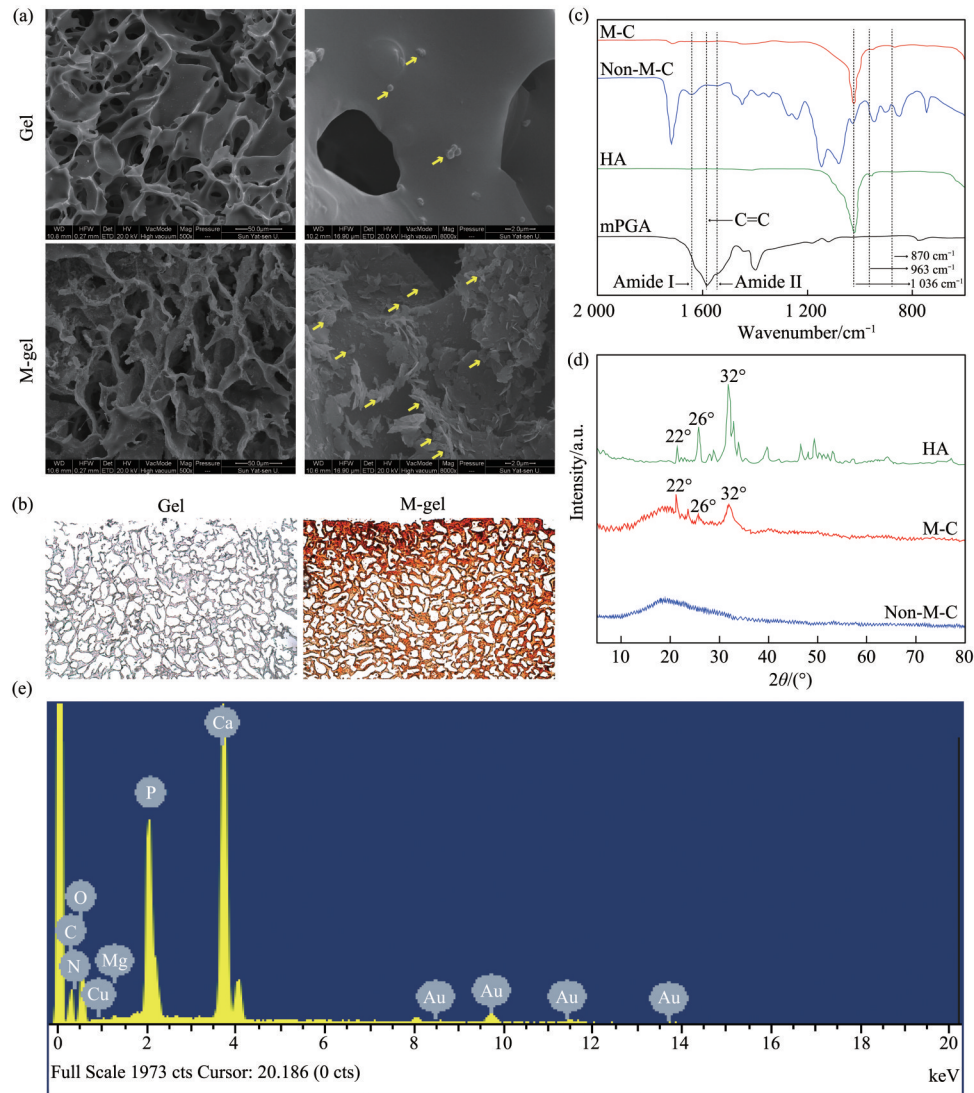


Fig. 3 Characterization of polymeric cryogel scaffolds

(a) SEM images of cryogel scaffolds (left: $\times 500$, right: $\times 8\ 000$). (b) Alizarin red S staining of cryogel scaffolds under optical microscopy. (c) FTIR spectra of mPGA and cryogels before and after mineralization. (d) XRD spectra of cryogels before and after mineralization. (e) SEM-EDS images of the mineralized cryogel scaffold.

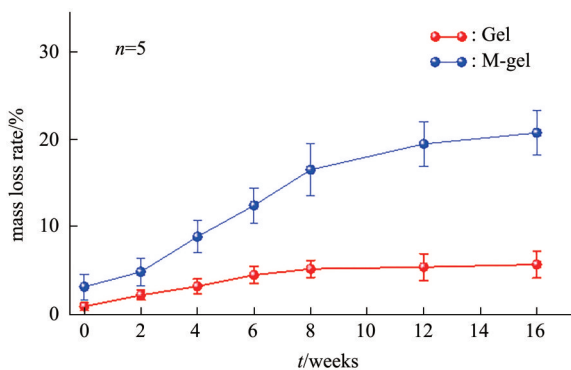


Fig. 4 Mass changes during degradation of cryogel in vitro

mineralized cryogel group was further increased ($P < 0.05$). It indicated that mineralization enhanced bone

regeneration in the orbital bone defect.

2.3 Angiogenesis in vivo

To further probe the changes in the orbital bone defect model microenvironment after implant surgery, we detected the expression of CD31 and α -SMA to evaluate the formation of new blood vessels. The expression of CD31 and α -SMA was less in the bone defect repair by the control group and the non-mineralized polymeric cryogel group (Figure 6). However, the co-localization of CD31 and α -SMA positive staining treated by the mineralized polymeric cryogel scaffolds group was significantly more than the other groups. The results demonstrated that the mineralized polymeric cryogel scaffolds had a

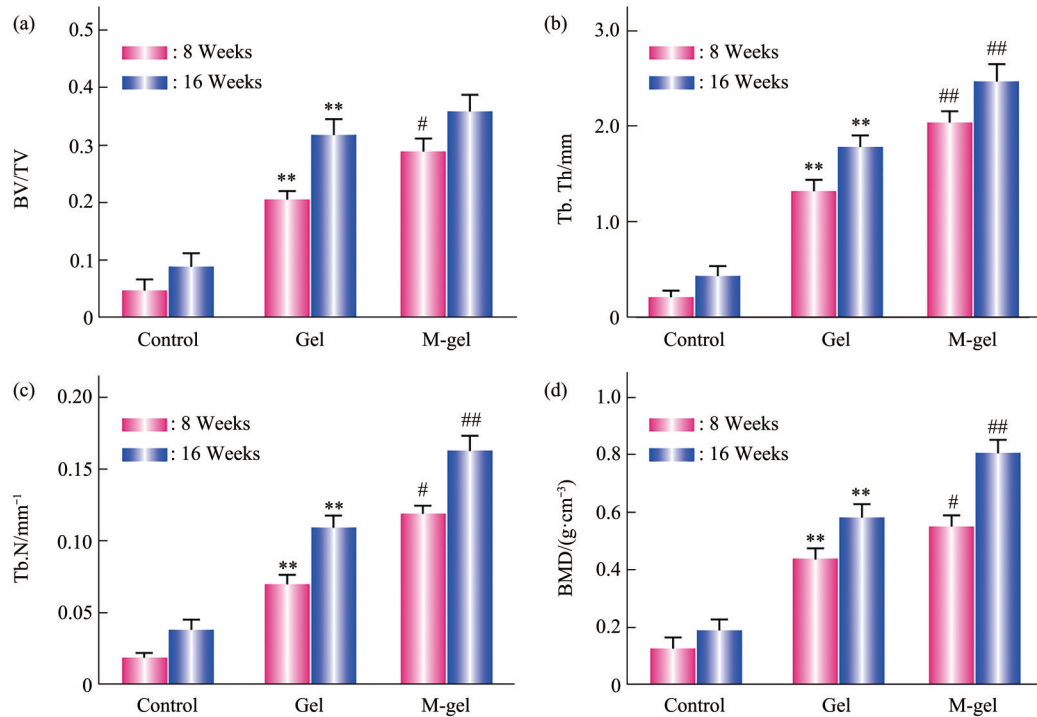


Fig. 5 Microstructure analysis of bone tissue in the defect sites

(a–d) Analysis of the bone volume/total volume (BV/TV), the trabecular bone thickness (Tb. Th), the trabecular bone number (Tb. N), and the bone mineral density (BMD) in the respective groups at 8 and 16 weeks post-surgery (for * $P < 0.05$ and ** $P < 0.01$ is Gel group vs. Control group, For # $P < 0.05$ and ## $P < 0.01$ is M-gel group vs. Gel group) (means±SD, $n=5$).

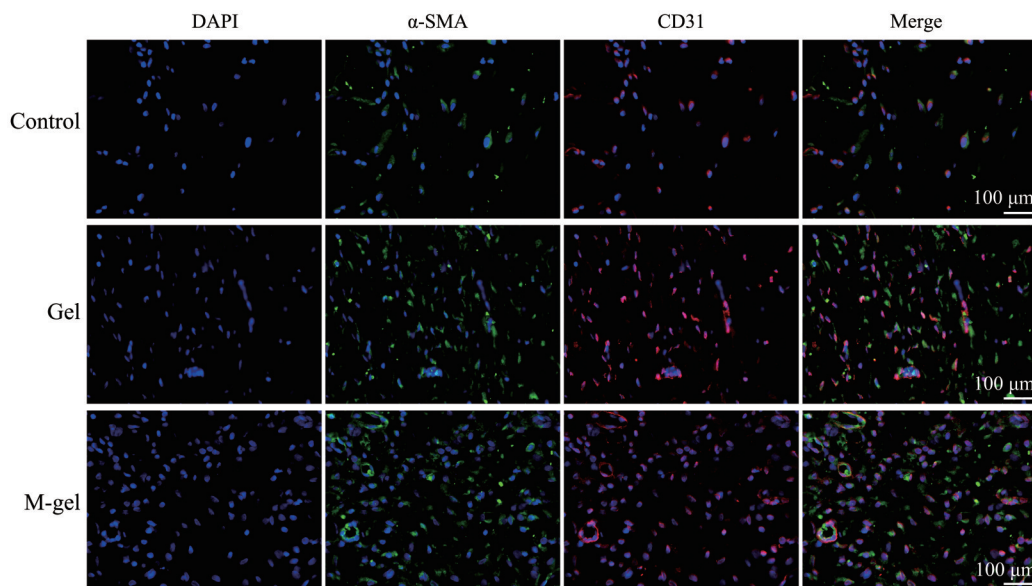


Fig. 6 Immunofluorescence staining of DAPI, CD31, and α -SMA in the orbital bone defect by implantation of Gel and M-gel scaffold for 8 weeks, respectively

significant effect on promoting angiogenesis during the bone defect repair process.

The FACS analysis suggested that CD31 protein expression was significantly increased in the

mineralized cryogel group compared with the non-mineralized group, indicating that the mineralized cryogel scaffolds have a positive regulatory role during angiogenesis. Obviously, the results suggest

that the mineralized polymeric cryogel scaffolds can promote endothelial cell overexpression of CD31 protein and consequently promote angiogenesis in the orbital defect region (Figure 7).

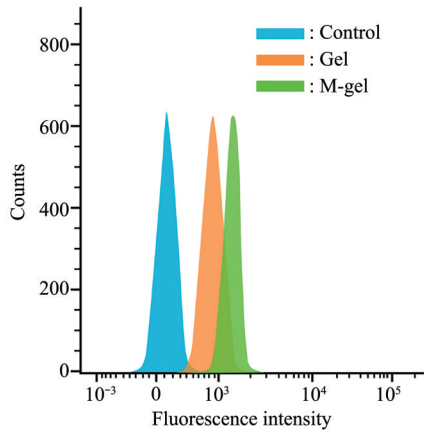


Fig. 7 Quantification fluorescence intensity of APC-conjugated CD31 treated with Gel and M-gel for 8 weeks were analyzed by flow cytometer

2.4 CT 3D reconstruction of the orbital defect

The morphology of newly formed bone is an important feature that is used to identify bone formation. The conditions of newly formed bones in the orbital bone defect site were detected with the CT 3D reconstruction technique. The 3D images (Figure 9a) described the different reparative effects of the three groups. No obvious bone formation was seen in the blank control group. Rabbits in Group B,

implanted with the non-mineralized polymeric cryogel scaffolds in the defect site, depicted bits of scattered newly formed bones at the edge of orbit. Rabbit in Group C in the defect site presented an obvious increase in newly formed bones compared with the other groups, which almost filled the whole orbital bone defect site.

2.5 H&E staining and immunohistochemical results

In order to detect the host response to the implant and the new bone formation, H&E staining and immunohistochemical staining were carried out to look into the bone regeneration conditions in the orbital bone defect sites. The H&E staining results showed that when compared with the control blank group (Group A), the polymeric cryogel scaffold groups (Group B, C) could significantly induce bone formation and matrix mineralization. In the orbital bone defect sites from the three groups, Group C showed regeneration of bone tissues, and even staining of newly formed bone tissues was noted. A certain amount of erythrocytes were observed inside and surrounding newly formed bones and scattered in new blood vessels. Group B displayed minimal regeneration of bone tissues except for some bone cells, and Group A showed no regeneration of bone tissue. While Group C displayed an even stronger mineralization ability than Group B. It was also noticed that the defect area was significantly reduced after 16 weeks (Figure 8).

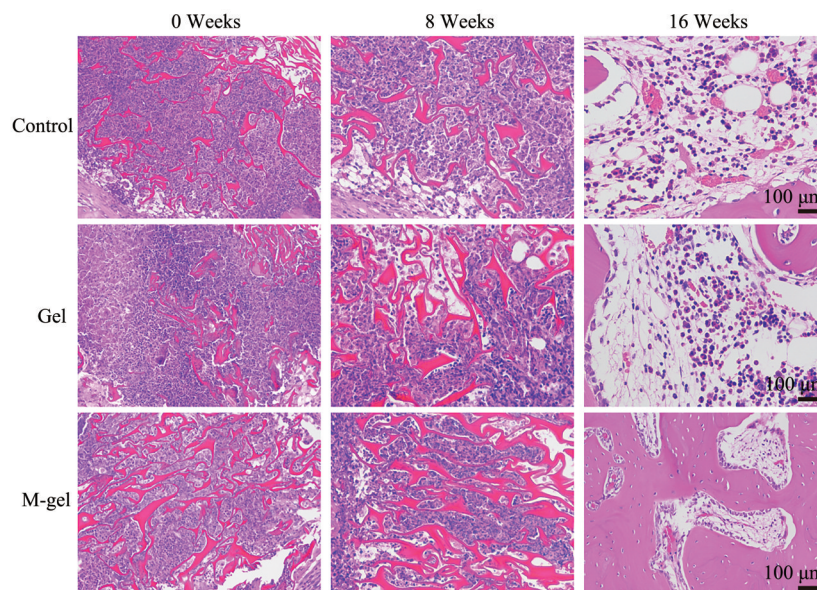


Fig. 8 Hematoxylin and eosin staining of orbital defect tissue sections after 0, 8, and 16 weeks implantation of the materials

In addition, we also examined the expression of osteogenic proteins of each group and found that positive staining of Runx-2, OPN, and ALP in cryogel scaffold groups increased notably as compared with

the control blank group. It's worth noting that the mineralized polymeric cryogel scaffolds further enhanced the ability (Figure 9b-e). It indicates that the mineralized polymeric cryogel scaffolds may

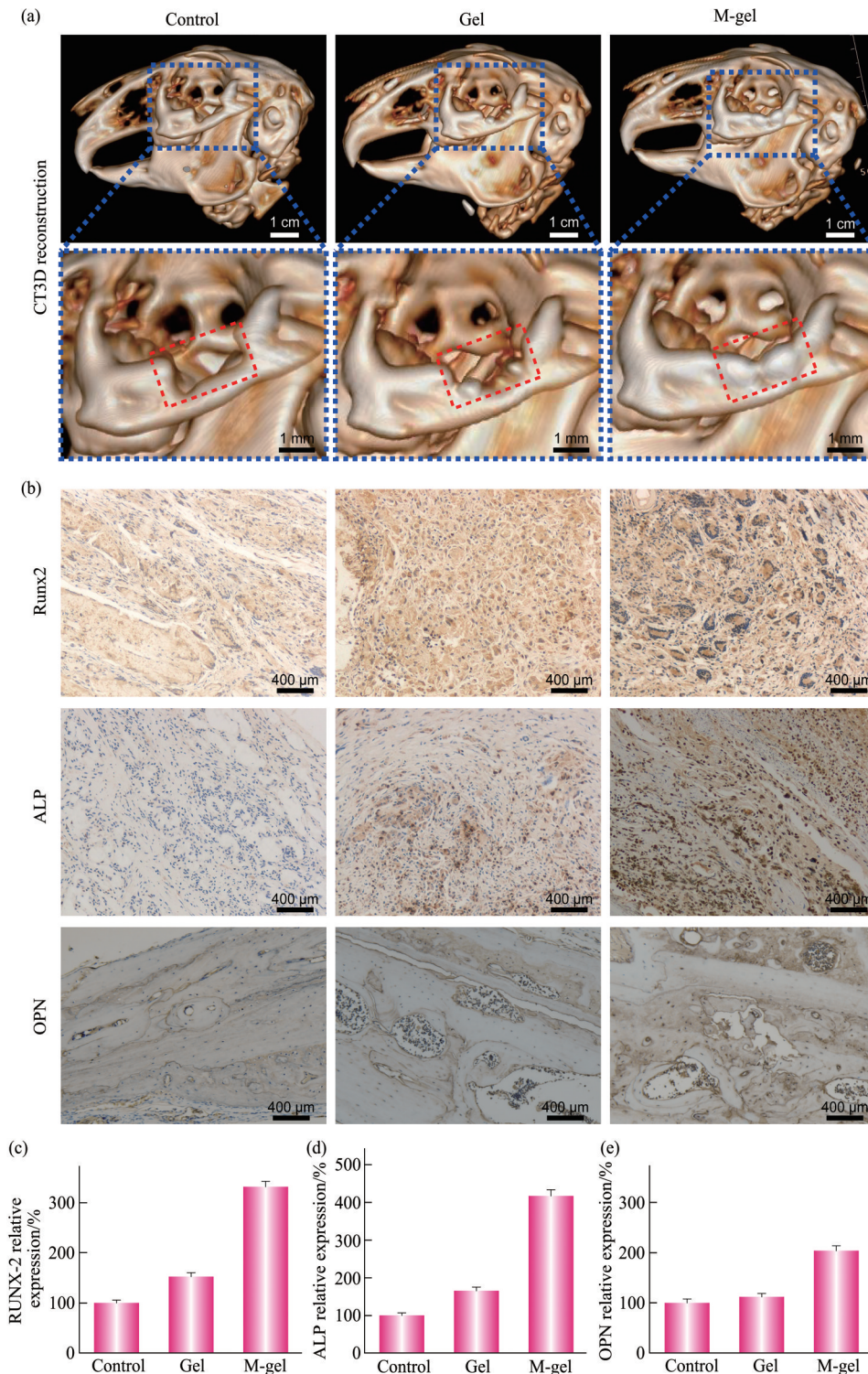


Fig. 9 M-gel promoted the repair of the orbital bone defects

(a) Comparison of the bone regeneration conditions in the orbital defect areas of rabbits from different groups detected by CT 3D reconstruction technique. Defect of the orbital bone (zygomatic bone) in the red frame. (b) Immunohistochemical analysis of bone regeneration at 16 weeks post-surgery. Optical photographs for immunohistochemical staining (Runx-2, ALP, and OPN) in sections of different groups. (c-e) Quantitative expression of immunohistochemical staining (Runx-2, ALP, and OPN).

promote bone regeneration during the repair of bone defects.

3 Discussion

The frontal, zygomatic, maxillary, sphenoid, ethmoid, palatine and lacrimal bones contribute to the structure of the orbit. Orbital bone fractures include fractures of these bones. With the increasing occurrence rates of the traffic accidents and industrial injuries in recent years, the incidence of orbital bone fracture defects also rises as well. The orbital bone defect is a common disease in ophthalmology clinics and a challenge in bone repair treatment as it is difficult to regenerate bone loss and reconstruct bone function. Although bone autograft and allograft have been extensively used in bone repair, there is the urge for the development of biomaterials that could not only overcome the shortcomings of autograft and allograft but also facilitate the regeneration/reconstruction of new bone tissue^[1, 3, 9].

To this end, polymeric cryogel with a unique interconnective porous structure and desired functionality may be harnessed as scaffolding materials in bone regeneration^[15]. The polymeric cryogel could be modified by various methods to acquire specific functions, *i. e.*, osteoinductivity and osteoconductivity. Mineralization has been a demonstrably effective and convenient method to introduce bioactivity and osteoinductivity to microporous scaffold materials. Previous *in vitro* studies^[17] have shown mineralized polymeric cryogel promotes osteogenic differentiation of mesenchymal stem cells (MSCs). The adsorption, entrapment, and concentration of vascular endothelial growth factor (VEGF) and bone morphogenetic protein 2 (BMP-2) in the matrices may participate in the process of angiogenesis and osteogenesis *in vivo*.

In this study, the polymeric cryogel maintains appreciable porosity and compressive modulus as well after mineralization. In addition, the higher mass loss rate of the mineralized cryogel scaffolds was evidenced, and the minerals deposited in the polymeric cryogel contain hydroxyapatite, carbonated apatite, and calcium phosphate, suggesting such the mineralized polymeric cryogel could be used as a potential bone tissue engineering material. Further studies *in vivo* are needed to prove the *in vitro* findings, the tests were performed by implanting the

polymeric cryogel scaffolds in rabbit orbital bone defects sites. Our study has confirmed that the implantation of the mineralized polymeric cryogel could promote osteogenesis in the animal orbital bone defect model at the studied time point. As for the non-mineralized polymeric cryogel scaffolds group, the microstructure analysis showed that much more new bones were detected in the mineralized polymeric cryogel scaffolds group, as confirmed by the quantificational results of the BV/TV, Tb. N, Tb. Th and BMD, indicating the mineralized cryogel scaffolds could repair the bone defect effectively. We observed that the new bone was almost filled the orbital bone defect in the mineralized polymeric cryogel scaffolds group in the image of CT 3D reconstruction. Angiogenesis is essential for the repair of bone defect. The results of immunofluorescence staining and flow cytometry demonstrated that the mineralized polymeric cryogel scaffolds could considerably accelerate the new bone formation. Histological analysis showed that in the control group, even though there was the minimum formation of new bone, the bony connection could not be detected and the defect area was filled by connective tissue, indicating the failure of repair of the defect. In comparison, the mineralized cryogel group achieved the significant formation of new bone tissue. In the meantime, the elevated staining of Runx-2, OPN, and ALP in the mineralized polymeric cryogel scaffolds group compared to the other groups unambiguously suggested the enhanced expression of osteogenic factors *in vivo*. The mineralized polymeric cryogel scaffolds used in the present study displayed admirable and positive histocompatibility and osteoinductivity, which could markedly enhance novel bone formation and bone regeneration when implanted into the orbital bone defect sites.

In the present study, the mineralized polymeric cryogel scaffolds were implanted into defect sites in rabbit models of orbital bone defects. Whereafter, the regeneration and volume of newly formed bones were demonstrated to be obviously increased compared with the control groups and non-mineralized cryogel groups. These analyses presented that mineralized polymeric cryogel had more extensive *in vivo* bone formation compared with non-mineralization. Multiple factors endow these positive outcomes. First, polymeric cryogel is characterized by appreciable protein adsorption and cell adhesion as a result of its

unique inter-connective porous structure, recruiting more osteoblasts to accelerate bone regeneration. What's more, mineralization played an indispensable role in osteogenic differentiation, which facilitated the new bone regeneration *in vivo*.

4 Conclusion

In brief, we developed the mineralized polymeric cryogel scaffolds as novel orbital bone repair biomaterials. The material had an inter-connective porous structure that enables fast transportation of nutrients, oxygen, and metabolite. The mineralized polymeric cryogel scaffolds had excellent biocompatibility. As compared with the non-mineralized polymeric cryogel scaffolds, the expression of osteogenic-related genes (Runx-2, OCN, and ALP) was remarkably up-regulated by the mineralized polymeric cryogel scaffolds. Additionally, the mineralized polymeric cryogel scaffolds accelerated bone regeneration and angiogenesis in the rabbit orbital defect sites. This study has demonstrated that mineralized polymeric cryogel scaffolds could be harnessed in the repair of orbital bone defects effectively, providing great clinical significance, and the novel material maybe has broader application in clinical practice.

References

- [1] Cruz A A, Eichenberger G C. Epidemiology and management of orbital fractures. *Curr Opin Ophthalmol*, 2004, **15**(5): 416-421
- [2] Bregman J A, Vakharia K T, Idowu O O, *et al*. Outpatient surgical management of orbital blowout fractures. *Craniofac Trauma Rec*, 2019, **12**(3): 205-210
- [3] Bratton E M, Durairaj V D. Orbital implants for fracture repair. *Curr Opin Ophthalmol*, 2011, **22**(5): 400-406
- [4] Jacono A A, Moskowitz B. Alloplastic implants for orbital wall reconstruction. *Facial Plast Surg*, 2000, **16**(1): 63-68
- [5] Horch H H, Pautke C. Regeneration instead of reparation: a critical review of the autogenous bone transplant as "golden standard" of reconstructive oral surgery. *Mund Kiefer Gesichtschir*, 2006, **10**(4): 213-220
- [6] Kelly C P, Cohen A J, Yavuzer R, *et al*. Cranial bone grafting for orbital reconstruction: is it still the best?. *J Craniofac Surg*, 2005, **16**(1): 181-185
- [7] Seiler J G, Johnson J. Iliac crest autogenous bone grafting: donor site complications. *J South Orthop Assoc*, 2000, **9**(2): 91-97
- [8] Hernigou P, Gras G, Marinello G, *et al*. Inactivation of HIV by application of heat and radiation: implication in bone banking with irradiated allograft bone. *Acta Orthop Scand*, 2000, **71**(5): 508-512
- [9] Potter J K, Ellis E. Biomaterials for reconstruction of the internal orbit. *J Oral Maxillofac Surg*, 2004, **62**(10): 1280-1297
- [10] Hicks C R, Morrison D, Lou X, *et al*. Orbital implants: potential new directions. *Expert Rev Med Devices*, 2006, **3**(6): 805-815
- [11] Lin I C, Liao S L, Lin L L. Porous polyethylene implants in orbital floor reconstruction. *J Formos Med Assoc*, 2007, **106**(1): 51-57
- [12] Tañag M A, Yano K, Hosokawa K. Orbital floor reconstruction using calcium phosphate cement paste: an animal study. *Plast Reconstr Surg*, 2004, **114**(7): 1826-1831
- [13] Bai X, Gao M Z, Syed S, *et al*. Bioactive hydrogels for bone regeneration. *Bioact Mater*, 2018, **3**(4): 401-417
- [14] Filmon R, Grizon F, Basle M F, *et al*. Effects of negatively charged groups (carboxymethyl) on the calcification of poly(2-hydroxyethyl methacrylate). *Biomaterials*, 2002, **23**(14): 3053-3059
- [15] Song J, Saiz E, Bertozzi C R. A new approach to mineralization of biocompatible hydrogel scaffolds: an efficient process toward 3-dimensional bonelike composites. *J Am Chem Soc*, 2003, **125**(5): 1236-1243
- [16] Song J, Malathong V, Bertozzi C R. Mineralization of synthetic polymer scaffolds: a bottom-up approach for the development of artificial bone. *J Am Chem Soc*, 2005, **127**(10): 3366-3372
- [17] Phadke A, Zhang C, Hwang Y, *et al*. Templated mineralization of synthetic hydrogels for bone-like composite materials: role of matrix hydrophobicity. *Biomacromolecules*, 2010, **11**(8): 2060-2068
- [18] Lozinsky V I, Galaev I Y, Plieva F M, *et al*. Polymeric cryogels as promising materials of biotechnological interest. *Trends Biotechnol*, 2003, **21**(10): 445-451
- [19] Kumar A, Plieva F M, Galaev I Y, *et al*. Affinity fractionation of lymphocytes using a monolithic cryogel. *J Immunol Methods*, 2003, **283**(1-2): 185-194
- [20] Liu C T, Tong G Q, Chen C Z. Polymeric cryogel: preparation, properties and biomedical applications. *Prog Chem*, 2014, **26**(7): 1190-1201
- [21] Liu C T, Liu X, Quan C Y, *et al*. Poly(γ -glutamic acid) induced homogeneous mineralization of the poly(ethylene glycol)-co-2-hydroxyethyl methacrylate cryogel for potential application in bone tissue engineering. *RSC Adv*, 2015, **5**(26): 20227-20233
- [22] Liu C T, Lin C W, Feng X R, *et al*. A biomimicking polymeric cryogel scaffold for repair of critical-sized cranial defect in a rat model. *Tissue Eng Pt A*, 2019, **25**(23-24): 1591-1604
- [23] Zeng W, Hu W K, Li H, *et al*. Preparation and characterization of poly(γ -glutamic acid) hydrogels as potential tissue engineering scaffolds. *Chinese J Polym Sci*, 2014, **32**(11): 1507-1514
- [24] Cai L, Wang S F. Poly(epsilon-caprolactone) acrylates synthesized using a facile method for fabricating networks to achieve controllable physicochemical properties and tunable cell responses. *Polymer*, 2010, **51**(1): 167-177
- [25] Oyane A, Kim H M, Furuya T, *et al*. Preparation and assessment of revised simulated body fluids. *J Biomed Mater Res A*, 2003, **65**(2): 188-195
- [26] 范先群,肖彩雯,周慧芳,等. 基因修饰的组织工程骨修复眶骨缺损的实验研究. *中华眼科杂志*, 2009, **45**(1): 66-72
- [27] Fan X Q, Xiao C W, Zhou H F, *et al*. *Chin J Ophthalmol*, 2009, **45**(1): 66-72
- [27] Gielkens P F, Schortinghuis J, de Jong J R, *et al*. A comparison of micro-CT, microradiography and histomorphometry in bone research. *Arch Oral Biol*, 2008, **53**(6): 558-566
- [28] Boussein M L, Boyd S K, Christiansen B A, *et al*. Guidelines for assessment of bone microstructure in rodents using micro-computed tomography. *J Bone Miner Res*, 2010, **25**(7): 1468-1486

γ -PGA/HEMA/PEG 聚合物晶胶支架修复兔眼眶骨折缺损的实验研究*

熊柯^{1,2)} 刘春桃¹⁾ 吴钊英¹⁾ 张伟^{3)**} 张超^{1)**}

(¹⁾ 中山大学生物医学工程学院, 深圳 518107;

²⁾ 南方医科大学南方医院眼科, 广州 510515; ³⁾ 中山大学附属第一医院门诊部, 广州 510080)

摘要 目的 近年来, 眼眶骨折发生率逐年增加, 其治疗关键旨在修复缺损的眼眶, 聚(γ -谷氨酸)/2-羟乙基甲基丙烯酸酯/聚(乙二醇)(γ -PGA/HEMA/PEG) 聚合物晶胶是一种具有互连多孔结构的新型支架材料, 研究旨在检验其在眼眶骨折缺损修复中的骨修复效果。**方法** 采用低温凝胶技术制备了 γ -PGA/HEMA/PEG 聚合物晶胶。制备了兔的眼眶骨缺损模型, 根据植入支架材料的不同分为3组, 空白对照组、聚合物晶胶组(Gel组)、矿化聚合物晶胶组(M-gel组)。植入后8周和16周标本取材进行大体观察, 通过影像学和组织学检查观察其血管生成和成骨效果。**结果** 影像学检查结果表明, 支架材料能有效促进眼眶缺损的修复, 缺损区被骨组织完全替代。组织学结果表明, 支架材料可以增加Runx-2(Runx-2)、碱性磷酸酶(ALP)、骨桥蛋白(OPN)和血小板内皮细胞黏附分子1(CD31)的表达, 这表明支架材料植入后血管生成和成骨能力增强。**结论** 矿化聚合物晶胶是一种良好的眼眶骨折缺损修复的支架材料。

关键词 修复, 眼眶骨折, 聚合物晶胶, 矿化, 成骨性

中图分类号 Q819, R777

DOI: 10.16476/j.pibb.2022.0309

* 广东省重点领域研究与发展计划(2020B090924004)和国家自然科学基金(81971760)资助项目。

** 通讯联系人。

张伟 Tel: 13556159255, E-mail: zhang8@mail.sysu.edu.cn

张超 Tel: 13751865819, E-mail: zhchao9@mail.sysu.edu.cn

收稿日期: 2022-07-01, 接受日期: 2022-07-28